

See discussions, stats, and author profiles for this publication at: <https://www.researchgate.net/publication/23401315>

Spectroscopic Characterization of Extracellular Polymeric Substances from *Escherichia coli* and *Serratia marcescens*: Suppression Using Sub-Inhibitory Concentrations of Bismuth Thiol...

ARTICLE in BIOMACROMOLECULES · NOVEMBER 2008

Impact Factor: 5.75 · DOI: 10.1021/bm800600p · Source: PubMed

CITATIONS

32

READS

98

7 AUTHORS, INCLUDING:



Appala Raju Badireddy

University of Vermont

36 PUBLICATIONS 949 CITATIONS

SEE PROFILE



Mark H Engelhard

Pacific Northwest National Laboratory

381 PUBLICATIONS 12,006 CITATIONS

SEE PROFILE



Scott Lea

Pacific Northwest National Laboratory

88 PUBLICATIONS 1,676 CITATIONS

SEE PROFILE



Kevin M. Rosso

Pacific Northwest National Laboratory

181 PUBLICATIONS 4,728 CITATIONS

SEE PROFILE

Spectroscopic Characterization of Extracellular Polymeric Substances from *Escherichia coli* and *Serratia marcescens*: Suppression Using Sub-Inhibitory Concentrations of Bismuth Thiols

Appala Raju Badireddy,[†] Bhoom Reddy Korpul,[†] Shankararaman Chellam,^{*,†,‡}
Paul L. Gassman,[§] Mark H. Engelhard,[§] Alan S. Lea,[§] and Kevin M. Rosso[§]

Department of Civil and Environmental Engineering, University of Houston, Houston, Texas 77204-4003,
Department of Chemical and Biomolecular Engineering, University of Houston, Houston,
Texas 77204-4004, and Environmental Molecular Sciences Laboratory, Pacific Northwest National
Laboratory, Richland, Washington 99352

Received May 30, 2008; Revised Manuscript Received August 16, 2008

Free and bound (or capsular) EPS produced by suspended cultures of *Escherichia coli* and *Serratia marcescens* were characterized in detail using colorimetric analysis of total proteins and polysaccharides, Fourier transform infrared spectroscopy (FTIR), X-ray photoelectron spectroscopy (XPS), and Auger electron spectroscopy (AES) in the presence and absence of bismuth-based antifouling agents. Subtle differences in the chemical composition of free and bound EPS were observed for both bacteria in the absence of bismuth. Total polysaccharides and proteins in free and bound EPS decreased upon treatment with subinhibitory concentrations of lipophilic bismuth thiols (bismuth dimercaptopropanol, BisBAL; bismuth ethanedithiol, BisEDT; and bismuth pyrithione, BisPYR), with BisBAL being most effective. Bismuth thiols also influenced acetylation and carboxylation of polysaccharides in EPS from *S. marcescens*. Extensive homology between EPS samples in the presence and absence of bismuth was observed with proteins, polysaccharides, and nucleic acids varying predominantly only in the total amount produced. Second derivative analysis of the amide I region of FTIR spectra revealed decreases in protein secondary structures in the presence of bismuth thiols. Hence, antifouling properties of bismuth thiols appear to originate in their ability to suppress O-acetylation and protein secondary structure formation in addition to free and bound EPS secretion.

Introduction

Bacteria secrete extracellular polymeric substances (EPS) to facilitate attachment with each other and to solid surfaces, protect themselves from predators and environmental stresses, communicate with other cells, and maintain hydration.^{1,2} EPS are predominantly comprised of polysaccharides, sugars, and proteins with smaller amounts of nucleic acids, (phospho)lipids, and humic-like substances. EPS are categorized as being either “free” or “bound” depending on whether they are released into the surrounding media or remain in close proximity to the cell surface. Free EPS has been shown to induce bacterial aggregation in suspended cultures³ and also form a conditioning film on surfaces prior to initial attachment.^{4,5} Cell–surface interactions are thought to be mediated by both bound and free EPS at the initial stages of biofilm formation.^{4,6,7} EPS production is also a crucial component of biofilms, which cause adverse consequences in technological systems by increasing resistances to heat and mass transfer and inducing higher pressure drops.⁵ Hence, there is much interest in developing strategies to mitigate EPS production, biofilm formation, and subsequent biological fouling.

One recently proposed approach is to employ bismuth thiols, which inhibit EPS production, exhibit antibacterial activity, and

have been shown to prevent biofilm formation in medical devices and membrane filters even at subminimum inhibitory concentrations (MIC).^{8–12} The requisite concentrations of bismuth when chelated with lipophilic thiols are ~1000-fold lower than those of elemental bismuth,⁹ thereby protecting mammalian host cells and reducing potential environmental hazards. Previous studies investigating the antifouling properties of bismuth thiols toward catheters⁸ and stents¹² mainly focused on capsular or bound EPS and only measured total polysaccharides and production of slime, which is a term used to describe the loosely bound polymers in biofilms.¹³ However, detailed chemical characterization of both free and bound EPS and all its constituents is essential to develop a rigorous understanding of bacterial aggregation and biofilm formation at the molecular level.^{3,6,11,14–16}

Fourier transform infrared (FTIR), X-ray photoelectron (XPS), and Auger electron spectroscopies (AES) can be employed to perform in-depth, molecular level characterization of EPS and biofilms. For example, FTIR has been applied to differentiate intact microbial cells based on the unique surface biochemistry of bacteria,^{17–19} to characterize EPS functionalities and conformations from pure cultures of *Pseudomonas* spp., *Brevundimonas diminuta*, and *Bacillus subtilis*, and even mixed bacterial cultures.^{6,11,14,20} The elemental composition and chemical functionalities of biomolecules on cell surfaces and the interactions of macromolecules of biological origin with a range of surfaces has also been studied using XPS.^{21–25} AES coupled with XPS has also been employed to investigate copper

* To whom correspondence should be addressed. Phone: (713) 743-4265. Fax: (713) 743-4260. E-mail: chellam@uh.edu.

[†] Department of Civil and Environmental Engineering.

[‡] Department of Chemical and Biomolecular Engineering.

[§] Pacific Northwest National Laboratory.

biocorrosion caused by exopolysaccharides secreted by *Pseudomonas atlantica*.²⁶ Even though overall biofilm formation and gross measures of EPS secretion (e.g., slime production and total polysaccharides by colorimetry) have been shown to decrease in the presence of bismuth thiols,^{8,10,12,27} detailed information on bismuth thiols' influence on individual EPS components is not yet available.

In this work, we characterize EPS produced by suspended cultures of two Gram negative bacteria: *Escherichia coli* and *Serratia marcescens*. *E. coli* is an important indicator for fecal contamination of water supplies and is capable of causing gastrointestinal diseases as well as extraintestinal infections.²⁸ *S. marcescens* has been recognized as a leading causative agent for nosocomial infection including respiratory tract infection, urinary tract infection, meningitis, and so on.²⁹ Additionally, clinical isolates of *S. marcescens* are often multidrug-resistant and can infect immunocompromised patients.^{29,30} *S. marcescens* is also the organism in the American Society of Testing and Materials challenge testing procedure to validate the sterilizing capability of membrane filters rated at 0.45 μm . Hence, all experiments were performed with these two bacteria as model organisms.

The overall goal of our research is to better understand the chemical basis of the antifouling properties of bismuth thiols. The specific objective of this study is to perform a comprehensive molecular and elemental characterization of both free and bound EPS secreted by suspended cultures of *S. marcescens* and *E. coli* in the presence and absence of three bismuth thiols (bismuth dimercaptopropanol, BisBAL; bismuth ethanedithiol, BisEDT; and bismuth pyrithione, BisPYR). EPS were extracted from planktonic bacteria primarily because it is known to mediate cell-surface interactions important during the initial stages of biofilm formation. Total polysaccharides and proteins were determined colorimetrically. FTIR was employed to characterize EPS composition and chemical functionalities. Quantitative analysis of the amide I (1700–1600 cm^{-1}) region was performed to determine protein secondary structures and their sensitivities to bismuth thiols. Elemental compositions (C, N, O, and P) were obtained by AES. XPS was also used to make measurements of atomic composition and functionality of EPS extracted from *S. marcescens*. Together, FTIR, XPS, and AES were employed to comprehensively characterize EPS functionalities, protein secondary structures, and elemental and chemical composition.

Experimental Section

All chemical solutions were prepared using ultrapure water from a Barnstead NANOpure system (Thermo Fisher Scientific, Inc., Waltham, MA) and chemicals were purchased from Sigma-Aldrich (St. Louis, MO).

Bacteria and Culture Conditions. Stock cultures of *S. marcescens* (American Type Culture Collection (ATCC) 14756) and *E. coli* (ATCC 25404), kept at -80°C were used for initial inoculation to prepare working cultures for all our experiments. *S. marcescens* was cultured in nutrient broth (Difco, Detroit, MI) at 26°C and *E. coli* was cultured in Luria-Bertani medium at 37°C overnight (~ 16 h) at 200 rpm in an orbital-shaker. The optical density (OD) at 600 nm of overnight cultures was adjusted to ~ 0.6 using the respective growth medium and then transferred to 250 mL conical flasks containing the medium with and without bismuth-thiols. A 60 mL culture was collected at the end of 2 days and 5 days for free and bound EPS extraction and analysis. As described in Results and Discussion, bacteria in these 2-day and 5-day samples were in the stationary growth phase. We focused on EPS secreted by planktonic bacteria because it is a crucial component

during the initial stages of cell attachment on surfaces before forming a mature biofilm.

Bismuth Thiol Preparation. Solutions of two bismuth dithiols (BisBAL and BisEDT) and one monothiol (BisPYR) were freshly made before each experiment by first preparing a 50 mM stock solution of $\text{Bi}(\text{NO}_3)_3$ by dissolving bismuth nitrate pentahydrate in propylene glycol (to increase the solubility). Next, 2.5 μL of 10 M 2,3-dimercapto-1-propanol (BAL), 2.3 μL of 10.7 M 1,2-ethanedithiol (EDT), and 250 μL of 0.1 M pyrithione were mixed separately with 1 mL $\text{Bi}(\text{NO}_3)_3$ stock solution in three separate glass vials to prepare BisBAL, BisEDT, and BisPYR, respectively. In all cases, a 2:1 molar ratio of bismuth to thiol was chosen since it remained stable over the 5-day duration of each experiment and has been previously investigated for biofilm control.^{8,10,11,31} Culture tubes containing 5 mL of growth medium spiked with 2:1 molar ratio bismuth thiol (0–20 μM) were inoculated with overnight cultures of *E. coli* or *S. marcescens* ($\sim 10^4$ CFU/mL) and incubated at 37°C or 26°C , respectively, while shaking at 200 rpm to determine the MIC for each thiol-bacteria combination. Propylene glycol concentration in the final solution containing bacteria, bismuth thiol, and the growth medium was $<0.05\%$ to prevent any potential interferences with bacterial growth.^{9,11} Each experiment designed to measure MICs was repeated at least three times.

²⁰⁹Bi concentrations in selected solutions were independently measured by inductively coupled plasma mass spectrometry (ICP-MS, Elan DRC II, Perkin-Elmer, Norwalk, CT) using a protocol similar to the one recently developed by us.³² Because bismuth has only one natural isotope, which is free of polyatomic interferences, the dynamic reaction cell was not employed and the instrument was operated in the standard mode. Before each measurement, a smart tune was performed first. Next, a multielement standard solution which includes 10 mg/L bismuth was used to prepare calibration standards by appropriate dilution based on the instrument's dynamic range. Three replicates were measured for each solution to quantify the precision. A fourth replicate was spiked with 0.1 μM of bismuth to determine the matrix spike recovery. In all cases, bismuth concentrations were within 5% of the target value with relative standard deviation $<2\%$ and spike recoveries between 95–105%. Hence, all BisBAL, BisPYR, and BisEDT concentrations reported in this manuscript are accurate and precise.

EPS Extraction. Free and bound EPS were extracted by first centrifuging 60 mL of bacterial culture (5000 g, 15 min, 4°C) to harvest cells from the growth media. The resultant supernatant consisted of free EPS along with any dissolved bismuth thiol and residual growth media, whereas the bound EPS was associated with the harvested cell pellet. The cell pellet collected after centrifugation was resuspended, washed once in isotonic buffer (10 mM Tris/HCl pH 8.0, 10 mM EDTA, 2.5% NaCl),¹⁴ and centrifuged (5000 g, 15 min, 4°C) again to remove any residual growth media from the cells. After washing, the cells pelleted by centrifugation were once again resuspended in 60 mL of isotonic buffer and incubated overnight at 4°C , after which the buffered cells were vortexed vigorously for 5 min prior to recovering the bound EPS as supernatant by centrifugation as described above. Adding EDTA efficiently recovers cell-bound EPS without decreasing cell viability or causing cell lysis.^{3,14,33,34}

The free and bound EPS were extracted from the respective supernatants by first centrifuging at 12000 g for 30 min at 4°C to remove any residual bacterial debris prior to the precipitation of EPS using ice-cold ethanol (99.5% purity) in a 1:3 sample-to-ethanol volume ratio.^{6,35} The suspensions were then stored at -20°C for ~ 18 h. Following incubation, free and bound EPS were recovered from suspensions in pellet form by centrifugation at 12000 g for 30 min at 4°C . The recovered EPS pellet was then dissolved in 10 mL of ultrapure water and dialyzed for 3 days against three changes of ultrapure water per day using regenerated cellulose 2000 Da molecular weight cutoff membranes (Spectra/Por7, Spectrum Chemicals, Gardena, CA) to remove bismuth thiols as well as ethanol and salts added during EPS extraction. The purified and concentrated EPS solutions were stored at -20°C until further analysis.

EPS Characterization. Free and bound EPS samples extracted from *E. coli* and *S. marcescens* cultures after 2 days, both in the presence and in the absence of bismuth thiols, were rigorously characterized in terms of total polysaccharides and proteins, elemental composition, chemical functionality, and protein secondary structures. Separate 5-day samples of bound and free EPS from bacteria in both the presence and the absence of bismuth were also analyzed by FTIR and total proteins and polysaccharides by colorimetry.

Total Proteins and Polysaccharides. Total proteins and polysaccharides were measured using standard colorimetric techniques.^{6,11} Proteins were determined using the Modified Lowry Protein Assay Kit (Pierce Biotechnology, Rockford, IL) with bovine serum albumin (BSA) standards. All samples were dialyzed using 2000 Da molecular weight cutoff membranes (Spectra/Por7, Spectrum Chemicals, Gardena, CA) prior to absorbance measurements at 750 nm to remove thiol and EDTA interferences. Polysaccharides were measured using the phenol-sulfuric acid method against glucose standards.

Fourier Transform Infrared Spectroscopy (FTIR). FTIR was employed to probe chemical and structural aspects of EPS as well as differences induced by bismuth thiol treatments. Spectra were collected using a Bruker IFS 66v/S FTIR spectrometer, equipped with a Globar source, KBr beam splitter, MCT detector and OPUS (v5.0) operating software. All spectra consist of 512 coadded scans collected at 4 cm⁻¹ resolution, with 16 cm⁻¹ phase resolution, and a zero-filling factor of 2 using a Blackman Harris three-term apodization and Mertz phase correction. A 16 kHz low-pass filter was used to prevent aliasing. The spectrometer was evacuated and stabilized at 7 mbar vacuum for 3 min before spectral collection to decrease strong absorbances from atmospheric CO₂ and water vapor.

Prior to FTIR analysis, a 9 mL sample of purified liquid EPS (free and bound) in ultrapure water was freeze-dried and ground with infrared grade KBr and encapsulated in KBr pellet and analyzed in transmission mode. Absorbance spectra were calculated as the ratio of the pellet spectrum against the open beam configuration. Each FTIR spectrum depicted in this manuscript is an average of 5 spectra.

Absorption band assignments in the region 1800–800 cm⁻¹ were based on vibration bands previously reported for bacteria and model proteins.^{11,36–38} Spectra were further analyzed in the amide I region (1700–1600 cm⁻¹) to extract information on protein secondary structures and potential changes upon exposure to different bismuth thiols. The amide I region was decomposed to separate overlapping peaks arising from distinct EPS components by enhancing spectral resolution.^{14,39,40} In this procedure, the second derivative of the original amide I spectra were obtained after nine-point Savitzky–Golay smoothing. Maximum absorption intensity, band frequency, and bandwidth, obtained from the second derivative spectra, were used to perform curve-fitting on the original spectra by assuming a Lorentzian shape for the amide I band and for each peak.

X-ray Photoelectron Spectroscopy (XPS). XPS (Physical Electronics Quantum 2000 Scanning ESCA Microprobe) was employed to obtain elemental composition and measure local functionality. XPS spectra were obtained only for 2-day bound and free EPS extracted from *S. marcescens* cultures. Measurements were performed on 20 μ L of air-dried EPS sample deposited on sputter cleaned 1 cm² pieces of a highly polished silicon wafer. The 20 μ L application and drying procedure was repeated in order to get a sufficiently thick film so as to minimize the signal from the silicon substrate. This system uses a focused monochromatic Al K α X-ray (1486.7 eV) source and a spherical section analyzer equipped with a 16 element multichannel detector. A 100 W, 100 μ m diameter X-ray beam was used and rastered over a 1.3 mm by 0.2 mm rectangle on the sample. The X-ray beam was incident normal to the sample and the photoelectron detector was at 45° off-normal. Wide scan (step size 1 eV) data was collected using a pass energy of 117.4 eV. For the Ag3d_{5/2} line, these conditions produced the full width at half-maximum (fwhm) of better than 1.6 eV. The high energy resolution (step size 0.1 eV) photoemission spectra were collected using a pass energy of 46.95 eV. For the Ag3d_{5/2} line,

these conditions produced fwhm of better than 0.98 eV. The binding energy (BE) scale was calibrated using the Cu2p_{3/2} feature at 932.62 \pm 0.05 eV and Au 4f at 83.96 \pm 0.05 eV for known standards. Because samples experienced variable degrees of charging, low energy electrons at \sim 1 eV, 20 μ A and low energy Ar⁺ ions were used to minimize this charging.⁴¹ XPS spectra depicted in this manuscript are the average of at least 10 spectra for each sample.

Auger Electron Spectroscopy (AES). Semiquantitative measurements of C, N, O, and P in free and bound EPS were obtained using AES. The 20 μ L aliquots of EPS samples were pipetted onto sputter cleaned 1 cm² pieces of a highly polished silicon wafer. The samples were allowed to air-dry and immediately introduced into the analysis chamber of a Physical Electronics 680 Auger electron spectrometer and examined using a 10 nA, 10 kV electron beam with a beam size of \sim 20 nm. This instrument is also equipped with a secondary electron detector that enables collection of electron micrographs to visualize the samples during analysis. No additional sample preparation was necessary to obtain electron micrographs. The beam was rastered over a sufficiently large area (609 \times 761 μ m) to obtain a representative EPS sample and to minimize damage by limiting the electron flux to the sample.^{42,43} Both wide scan (survey) and narrow scan (multiplex) spectra were collected on each of the samples. For quantitation, the multiplex spectra were subjected to a Savitzky–Golay 9-point smoothing and 5-point differentiation process. The resultant peak-to-peak heights were converted to atomic concentrations using standard sensitivity factors.⁴⁴ In some instances, in situ secondary electron images of the EPS samples were collected. Each spectrum reported in this manuscript represents the average of at least 10 spectra for every sample.

Results and Discussion

Effects of Bismuth Thiols on Growth. The effects of bismuth thiols on optical densities averaged from three separate experiments for each bacterial culture following 24 h of growth are shown in Figure 1. In all cases, a threshold bismuth thiol concentration was observed below which bacterial growth was not affected whereas at higher concentrations growth was inhibited. The MICs (defined as the lowest bismuth thiol concentration that inhibited growth for a 24 h period) of BisBAL, BisEDT and BisPYR for *S. marcescens* were in the range 5–7, 2–3, and 7–10 μ M, respectively and, similarly, MICs for *E. coli* were in the range 11–12, 6–7, and 5–7 μ M, respectively. These MICs correspond closely to the range of values reported previously for Gram-negative bacteria including other *E. coli* and *S. marcescens* strains.^{8,9,11,27}

Next, experiments were conducted using bismuth thiols at sub MICs (5 μ M BisBAL, 2 μ M BisEDT, and 7 μ M BisPYR for *S. marcescens* and 11 μ M BisBAL, 6 μ M BisEDT, and 5 μ M BisPYR for *E. coli*) to investigate EPS inhibition without bacterial inactivation after 2 days and 5 days of growth. This approach allowed a comparison of the EPS inhibitory capabilities of different thiols while maintaining the same number concentrations of viable bacteria and simultaneously achieving the greatest possible reductions in EPS levels. Additionally, during in vitro studies, lower concentrations (sub-MICs) are better tolerated by mammalian cells³¹ and also decrease potential environmental impacts compared with dosages greater than the MIC.

Figures S1a and S1b of the Supporting Information depict growth curves for *S. marcescens* and *E. coli*, respectively, in controls and in the presence of sub-MICs of bismuth thiols. Both bacteria followed typical batch growth profiles in which the exponential phase lasted for 10 h, the stationary phase started at 20 h, and bismuth thiols did not influence growth kinetics for the entire 5-day growth period. CTC-formazan and DAPI stained cells were also visualized using epifluorescence micros-

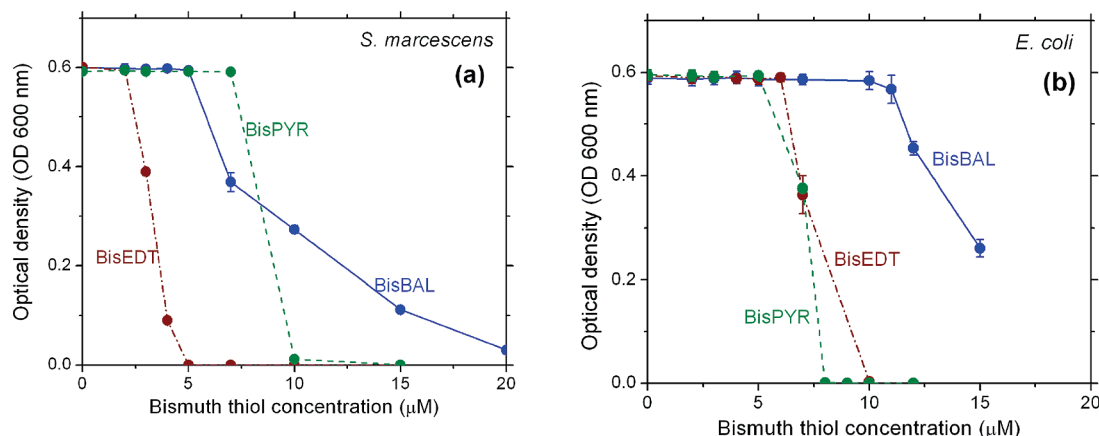


Figure 1. Effect of various bismuth thiols on the 24 h growth of *S. marcescens* (a) and *E. coli* (b) to determine the minimum inhibitory concentrations.

Table 1. Total Polysaccharides and Proteins in Bound and Free EPS Produced by Stationary-Phase Cultures of *S. marcescens* and *E. coli*

sample	2 days of growth (mg/g dry cells)				5 days of growth (mg/g dry cells)			
	bound EPS		free EPS		bound EPS		free EPS	
	polysaccharides	proteins	polysaccharides	proteins	polysaccharides	proteins	polysaccharides	proteins
Stationary-Phase Cultures of <i>S. marcescens</i>								
control	17.41 ± 2.74	13.22 ± 3.19	42.73 ± 5.91	30.40 ± 1.51	30.24 ± 2.38	22.76 ± 1.98	92.53 ± 1.03	58.06 ± 4.00
BisBAL	2.93 ± 0.78	1.32 ± 0.57	3.38 ± 1.35	2.96 ± 0.99	2.03 ± 0.68	1.65 ± 0.57	6.10 ± 1.36	5.28 ± 1.51
BisEDT	3.40 ± 0.68	2.32 ± 1.15	10.42 ± 1.96	4.96 ± 0.99	6.55 ± 1.70	6.27 ± 1.14	12.64 ± 2.56	8.58 ± 1.51
BisPYR	4.07 ± 1.79	5.95 ± 0.99	12.89 ± 1.17	6.61 ± 2.06	9.27 ± 2.74	8.92 ± 0.99	37.53 ± 2.74	18.83 ± 1.98
Stationary-Phase Cultures of <i>E. coli</i>								
control	23.38 ± 1.56	15.20 ± 2.37	42.08 ± 2.81	86.20 ± 7.32	35.52 ± 2.38	23.11 ± 2.37	57.30 ± 2.38	143.88 ± 1.59
BisBAL	3.11 ± 0.78	1.90 ± 0.66	5.48 ± 1.52	7.59 ± 1.74	3.90 ± 0.78	2.66 ± 0.66	7.28 ± 1.19	9.12 ± 1.14
BisEDT	7.03 ± 0.78	4.18 ± 1.32	8.85 ± 0.45	9.89 ± 2.87	8.05 ± 1.19	9.10 ± 1.14	12.46 ± 2.06	23.90 ± 2.28
BisPYR	8.32 ± 1.19	5.32 ± 0.66	20.28 ± 2.06	48.70 ± 5.14	15.05 ± 2.50	12.14 ± 1.74	13.24 ± 1.56	24.65 ± 5.38

copy to determine the viability of *S. marcescens* and *E. coli* (see Figures S2 and S3 and Tables S1 and S2 of the Supporting Information). As observed, the fraction of metabolically active cells remained constant at approximately 35% for the 2-day and 5-day samples of both bacteria. Also, the presence of sub-MICs of BisBAL, BisEDT, and BisPYR did not significantly change the respiratory activity of both bacteria during the stationary phase. Additionally, it should be noted that in all cases the same volume (60 mL) of bacterial culture was used to obtain EPS extractions. Therefore, all measurements reported herein for the 2-day and 5-day samples correspond to EPS produced by approximately the same total number and viable number of bacteria in the stationary phase.

Total Polysaccharides and Proteins. Table 1 summarizes the influence of bismuth thiols on total polysaccharides and proteins in free and bound EPS produced by *S. marcescens* and *E. coli*, respectively. Bound and free EPS samples were each analyzed in triplicate and the mean and standard deviations are reported after normalizing by the dry cell mass.

As observed in Table 1, concentrations of free and bound polysaccharides and proteins increased with time in the control samples (no bismuth). The total (polysaccharides + proteins) free EPS was always higher than total bound EPS. In other words, both bacteria secreted copious amounts of free EPS compared with bound EPS similar to earlier reports using *B. subtilis*,⁶ *B. diminuta*,¹¹ and *E. coli* MG1655.³ In the absence of bismuth thiols, the polysaccharide content of bound and free EPS of *S. marcescens* and bound EPS of *E. coli* was consistently higher than protein content for both the 2-day and 5-day samples. However, free EPS produced by *E. coli* contained higher concentrations of protein than polysaccharides potentially

due to shedding their outer membrane proteins.^{3,45} Substantial reductions in total (free + bound) EPS were achieved for both bacteria following exposure to bismuth thiols with the efficacy decreasing as BisBAL > BisEDT > BisPYR under our experimental conditions. BisBAL was highly effective, decreasing total EPS (polysaccharides and proteins in free and bound EPS) production in *S. marcescens* and *E. coli* by >90% similar to previous reports for both planktonic and sessile bacteria.^{10–12,27,31}

Fourier-Transform Infrared Spectroscopy (FTIR). Band assignments for mid-infrared EPS spectra given in Table 2 are based on previous reports for bacteria and model organic compounds.^{36,37,46} Information on the composition and functionality of EPS constituents was extracted from the region 1800–800 cm^{−1}. In general, the amide I (1700–1600 cm^{−1}), amide II (1600–1500 cm^{−1}), and amide III (1300–1200 cm^{−1}) ranges are all associated with proteins, whereas 1200–900 cm^{−1} is attributed to polysaccharides and nucleic acids.

FTIR spectra of free and bound EPS samples extracted from cultures after 2 days and 5 days of incubation and in the presence and absence of bismuth thiols for *S. marcescens* and *E. coli* are shown in Figures 2 and 3, respectively. Similar to our recent report for *B. diminuta*¹¹ and consistent with results summarized in Table 1, the dominant effect of bismuth thiols treatments for *S. marcescens* and *E. coli* was to decrease production of both free and bound EPS as determined by infrared absorbance intensities. Bismuth thiols had a negligible effect on the homology of EPS constituents as evidenced by the very similar FTIR spectral signatures (for free and bound EPS of both bacteria). Dithiols (BisBAL and BisEDT) were more effective (largest suppression by BisBAL) than the monothiol (BisPYR)

Table 2. Band Assignments for FTIR Spectral Features (cm^{-1}) of Bound and Free EPS^{36,37,46}

bound EPS	free EPS	band assignments
1741	1739	C=O stretch, esters, O-alkyl group
1633	1643	ν_s C=O stretch (amide I) associated with proteins; NH_2 scissors of primary amines
	1550	δ N-H and ν_s C-N stretches (amide II) associated with proteins
1457	1454	δ C-OH and δ_s CH_3 , δ_s CH_2 possibly associated with proteins
1403	1405	ν_s COO^- stretches associated with amino acids
1384	1384	ν_s C-O stretching of COO^- groups
1363	1357	ν_s C-O and δ C-H stretches possibly associated with amino acids
1326	1326	δ C-H stretches associated with amines and lipids
1236	1241	ν_s C-N stretch associated with secondary amides of proteins (amide III)
1209	1205	ν_{as} P=O from either nucleic acids or phosphorylated proteins; may also be due to δ N-H, δ C-H, ν_s C-N, and ν_s C-C
1157	1155	δ C-OH, δ C-O, and ν C-O possibly associated with amino acids
1114, 1080	1112, 1078	ring vibrations ν P=O, ν C-O-C, ν C-O-P as in phosphodiester and polysaccharides
1043	1035	ν C-OH of phosphorylated proteins and associated alcohols
956	952	ν_{as} O-P-O stretches associated with nucleic acids
916	916	ν_s C-O-C associated with aliphatic ethers
858	862	ring "breathing" associated with ν C-C and ν C-OH

in EPS suppression because they are better chelators, are more lipophilic, and consequently are better absorbed by bacteria.^{8-10,31} Also, 2- and 5-day spectra for both free and bound EPS were homologous for individual bacteria, indicating negligible changes in chemical composition once stationary phase had been reached. As may be expected,^{3,11,27} higher absorbances were measured after 5 days compared with 2 days in the absence of bismuth thiols, in control samples, indicating greater production of bound and free EPS with time.

Several common features were observed in all FTIR spectra (2- and 5-day, free and bound EPS, and *S. marcescens* and *E. coli*) demonstrating the presence of polysaccharides, proteins, phospholipids, and nucleic acids in EPS. Vibrations between 1741 and 1727 cm^{-1} were attributed to $\nu\text{C=O}$ of O-acetyl esters bonds. The band at 1633 cm^{-1} was specifically assigned to β -pleated sheet structures of proteins in the amide I region. Peaks in the region 1470–1300 cm^{-1} were primarily due to the bending vibrations of $-\text{CH}_3$, $-\text{CH}_2$, and $-\text{CH}$ groups from polysaccharides and proteins. The peak at 1403 cm^{-1} is associated with $\nu_s\text{C-O}$ of carboxylate groups. Bands in the region 1310–1240 cm^{-1} were contributions from amide III. The region 1250–1220 cm^{-1} is associated with $\nu_{as}\text{P=O}$ of POO^- of phosphodiester. The peak at 1080 cm^{-1} is caused by $\nu\text{P=O}$ of phosphoryl and phosphodiester groups from phosphorylated proteins, phosphate products, and nucleic acids. Band vibrations in the region 1200–900 cm^{-1} attributed to $\nu\text{C-C}$, $\nu\text{C-O}$, $\delta\text{C-O-H}$, and $\delta\text{C-O-C}$ vibrations were mainly due to carbohydrates. The region 900–800 cm^{-1} corresponds to secondary amines.

Differences were also observed in the chemical composition of free and bound EPS constituents for both bacteria. The amide

II peak at 1550 cm^{-1} , due to $\delta\text{NH}/\nu\text{C=O}$ of proteins, was found only in free EPS (Figures 2b,d, and 3b,d). Peaks in the 1200–900 cm^{-1} range were more intense in free EPS suggesting that it was relatively enriched in neutral carbohydrates compared with cell-bound EPS. Analogously, intense amide I peaks indicate important contributions from proteins to bound EPS. Similar to *Pseudomonas* spp.,¹⁴ both free and bound EPS consist of acidic moieties, as suggested by a peak at 1403 cm^{-1} (especially in the absence of bismuth), which indicates the presence of constituents with COO^- groups. Additionally, the peaks at 1554 cm^{-1} (coupled $\nu(\text{C=O})$ and $(\delta\text{N-H})$ in amides) and 1240 cm^{-1} (due to the P=O bond vibrations from phosphodiester of nucleic acids) were present in free EPS but were absent in bound EPS. These data suggest higher concentrations of nucleic acids in free EPS compared to bound EPS for both *E. coli* and *S. marcescens*.

Absorbances at 1739 cm^{-1} (symmetric C=O stretches associated with O-acetyl ester bonds) and 1240 cm^{-1} (C-O-C) were significantly decreased by bismuth treatment for both free and bound EPS from *S. marcescens*. Hence, similar to *B. diminuta*¹¹ and *Pseudomonas aeruginosa*,⁴⁷ inhibition of carbohydrate O-acetylation is a potential mechanism by which bismuth thiols inhibit fouling by *S. marcescens*. In contrast, the peak at 1739 cm^{-1} was insignificant for *E. coli* (similar to another recent report³) and bismuth thiols were therefore effective only in decreasing the peak intensity at 1240 cm^{-1} , which was especially prominent in free EPS. This suggests that components other than O-acetylated carbohydrates maybe important for *E. coli* biofilms.

Quantitative analysis of dominant FTIR bands viz. amide I, amide II, and COO^- for free and bound EPS from 2-day and 5-day samples of *E. coli* was also performed. Percentage reductions of band areas caused by bismuth thiols relative to the control values (no bismuth) are summarized in Table 3. As expected from Figures 2 and 3, dithiols were generally more effective than the monothiol in decreasing EPS production. The largest decreases in EPS proteins were obtained using BisBAL; 80% for bound EPS and 94% for free EPS. Reductions summarized in Table 3 from individual FTIR bands are similar in magnitude with our recent colorimetric measurements of total proteins for *B. diminuta*¹¹ and results shown in Table 1.

Effects of Bismuth Thiols on Protein Secondary Structures. More detailed analysis of EPS protein secondary structures was undertaken by obtaining the derivative spectra (Figure 4), which was subsequently used to curve-fit the amide I band of the original spectra (Figures 2 and 3).^{14,39,48} Table 4 summarizes the secondary structures present in free- and bound EPS obtained by the curve-fitting procedure for *S. marcescens* and *E. coli* for the 2-day samples. Secondary structures were assigned using well accepted amide I wave numbers based on spectral analysis of model peptides and proteins of known structures.^{14,40}

As seen in Table 4, bound and free EPS of both bacteria were contained predominantly in β -sheets (including unordered structures or random coils) and α -helices, with 3-turn helices and aggregated strands as minor constituents. Generally, EPS were richer in β -sheets compared with α -helices except for free EPS from *E. coli* where the reverse was observed. Bismuth treatment significantly decreased secondary structure concentrations in *E. coli* and *S. marcescens*; BisBAL giving the largest (77–88%) reductions and BisPYR being least effective (53–68%). These changes in protein secondary structures induced by exposure to sub inhibitory concentrations of bismuth thiols can inhibit adsorption to mineral surfaces.⁶

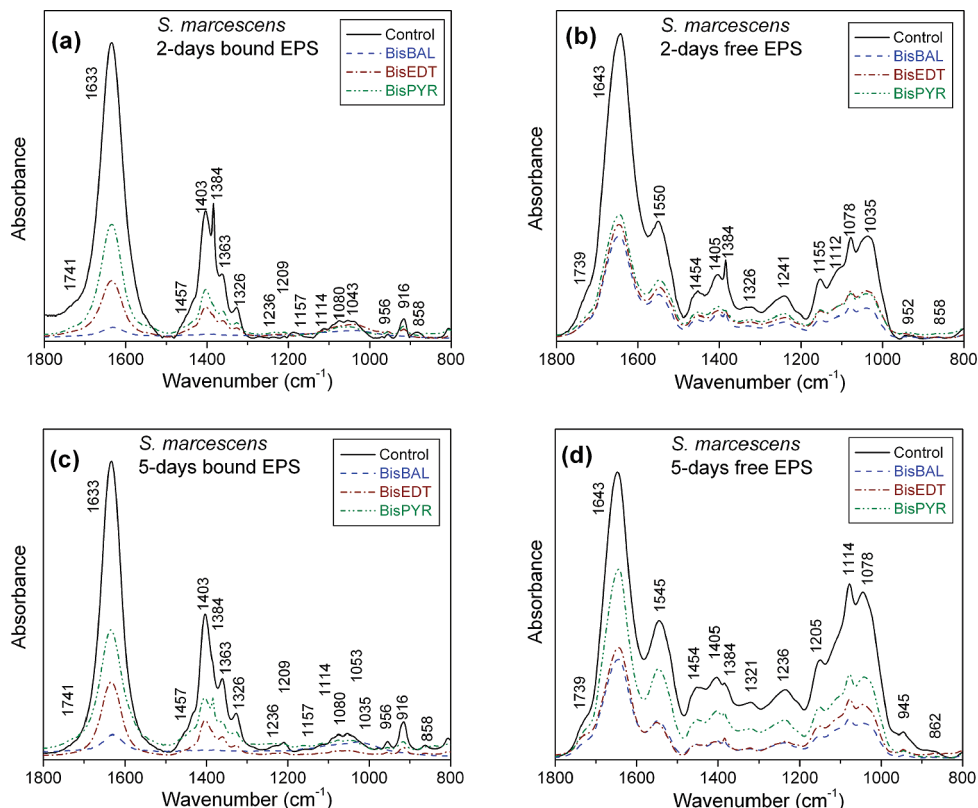


Figure 2. FTIR spectra of bound and free EPS extracted from stationary phase *S. marcescens* cultures in the presence and absence of bismuth thiols. Bound and free EPS produced after 2 days of incubation are shown in (a) and (b), respectively, whereas 5-day EPS samples are depicted in (c) and (d). Controls (without bismuth treatment) and bismuth-treated samples were both obtained after 2 days (a and b) and 5 days (c and d).

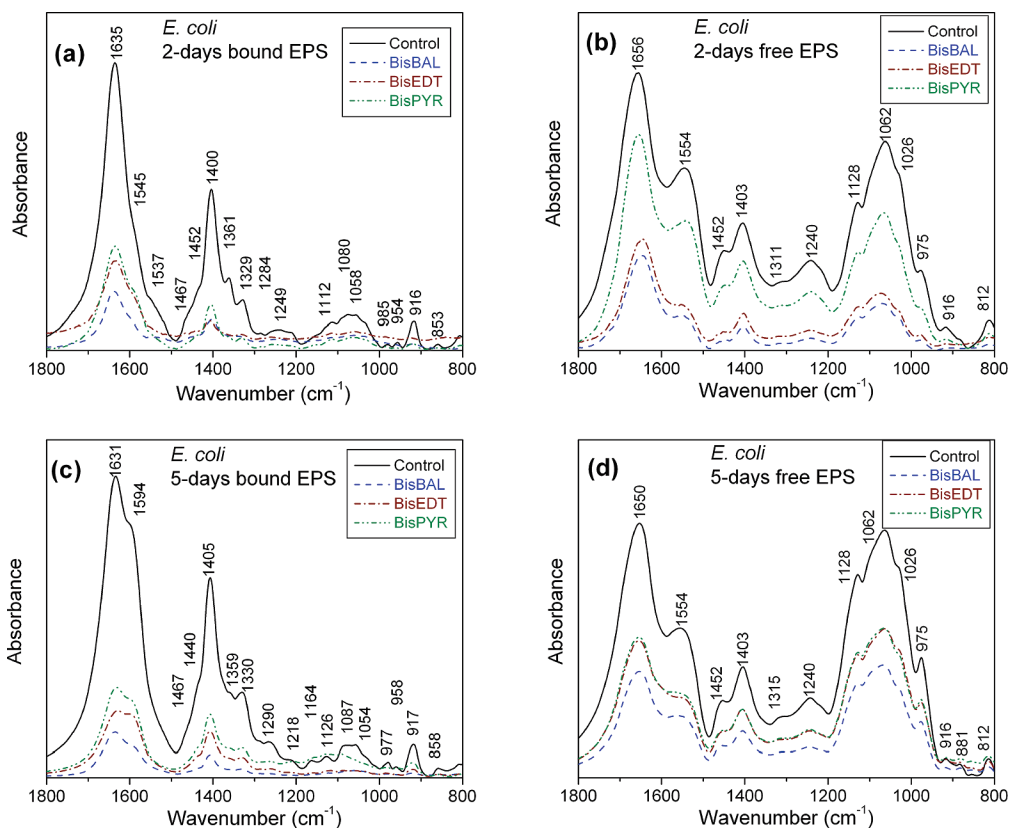
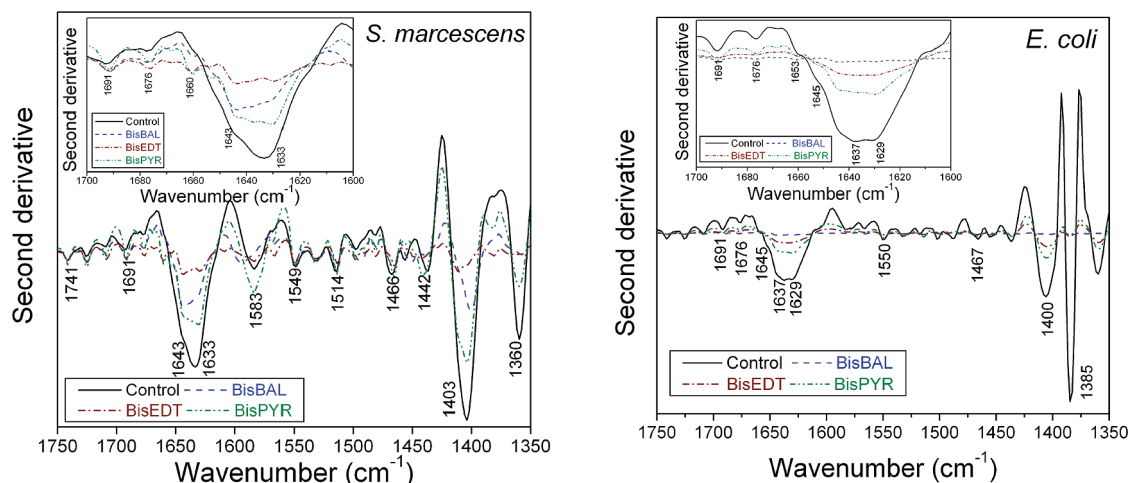


Figure 3. FTIR spectra of bound and free EPS extracted from stationary phase *E. coli* cultures in the presence and absence of bismuth thiols. Bound and free EPS produced after 2 days of incubation are shown in (a) and (b), respectively, whereas 5-day EPS samples are depicted in (c) and (d). Controls (without bismuth treatment) and bismuth-treated samples were both obtained after 2 days (a and b) and 5 days (c and d).

Table 3. Effects of Bismuth Thiols on Bound and Free EPS Band Areas for *E. coli* after 2 Days and 5 Days of Growth^a

band	2 days of growth						5 days of growth					
	BisBAL		BisEDT		BisPYR		BisBAL		BisEDT		BisPYR	
	bound	free	bound	free	bound	free	bound	free	bound	free	bound	free
amide I	81	92	69	92	66	34	92	94	89	89	66	86
amide II	63	96	30	95	75	29	33	93	30	75	25	75
COO ⁻	87	97	61	95	75	33	97	87	81	75	75	75

^a Percentage reductions of band areas relative to control values are shown.**Figure 4.** Second derivative spectra for bound EPS from 2-day cultures of *S. marcescens* and *E. coli*. The amide I region (1600 – 1700 cm⁻¹) is shown separately in the insets for clarity.**Table 4.** Effects of Bismuth Thiols on EPS Protein Secondary Structures for a 2-Day *S. marcescens* and *E. coli* Culture from Derivative Spectra and Curve Fitting

secondary structures	wavenumber (cm ⁻¹)	bound EPS				free EPS			
		control (no bismuth; %)	BisBAL ^a	BisEDT ^a	BisPYR ^a	control (no bismuth; %)	BisBAL ^a	BisEDT ^a	BisPYR ^a
		2-Day <i>S. marcescens</i> Culture				2-Day <i>E. coli</i> Culture			
aggregated strands	1625–1610	7.0				8.0	2.2	3.5	5.0
β-sheet	1640–1630	36.0	5.8	7.0	7.8	38.0	7.8	12.1	16.2
unordered	1645–1640	28.0	7.8	10.0	13.8	33.0	9.2	11.4	15.0
α-helix	1657–1648	17.0	3.7	4.4	5.0	11.0	2.8	3	4.3
3-turn helix	1666–1659	9.0	3.3	4.8	5.2	3.0			
antiparallel	1680–1695	3.0				7.0	0.5	1.7	2.4
β-sheet/aggregated strands									
aggregated strands	1625–1610					5.0	0.3	1.5	2.3
β-sheet	1640–1630	37.0	4.3	8.0	16.0	17.0	5.0	6.8	7.2
unordered	1645–1640	33.0	5.0	12.4	15.2	25.0	5.7	8.0	12.0
α-helix	1657–1648	27.0	3.0	5.0	9.5	42.0	11.2	17.8	22.0
3-turn helix	1666–1659	1.0				7.0		0.9	1.7
antiparallel	1680–1695	2.0				4.0		1.1	2.0
β-sheet/aggregated strands									

^a Values for the bismuth-treated samples denote the percentages with respect to the respective control value.

X-ray Photoelectron Spectroscopy (XPS). Figure 5 shows the XPS spectra collected in the energy range 0–1200 eV for 2-day samples of bound and free EPS of *S. marcescens* in the presence and absence of bismuth thiols. XPS spectra were also largely homologous confirming FTIR results that the primary effect of bismuth thiol treatment is to decrease elemental concentrations in EPS while preserving its overall composition. Similar to FTIR spectroscopy and earlier reports for *P. aeruginosa*,³¹ and *Staphylococcus* spp.⁸ Figure 5 suggests that BisBAL was more effective than other bismuth thiols in inhibiting both bound and free EPS production for *S. marcescens* and *E. coli* (also see O/C ratios in Table 5). Again, consistent with Figures 2 and 3, lower counts were obtained for BisBAL and BisEDT (dithiols) than BisPYR (monothiol). The core-level peaks were

C 1s (284.8 eV), O 1s (532.0 eV), and N 1s (400.0 eV), with a minor peak associated with P 2p (133.4 eV). Si and Na peaks in Figure 5 were most likely due to the silicon substrate and buffer used.

Because elemental peak positions depend on the functional groups associated with them,⁴⁹ high resolution scans of C 1s, O 1s, and N 1s were obtained as the first step in obtaining detailed information on their chemical functionality (Figure 6).^{23,24,41,49} Because XPS spectra upon bismuth treatment were largely homologous in terms of functionalities of EPS constituents with control samples (no bismuth), peak decomposition results were essentially the same regardless of bismuth thiols addition. Therefore, Figure 6 depicts C, N, and O deconvolution results only for the controls. Also, only BisBAL was chosen

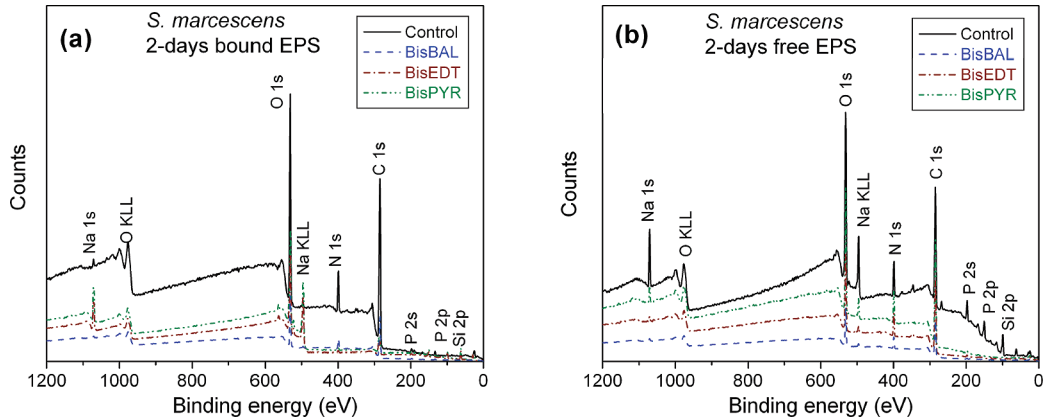


Figure 5. XPS wide survey scans of EPS from *S. marcescens* after 2 days of incubation. Bound EPS is shown in (a) and free EPS is shown in (b).

Table 5. Effects of BisBAL on N, O, and P Atomic Ratios and Functional Groups with Respect to C from High Resolution XPS Spectra Used To Quantify 2-Day EPS Extracted from *S. marcescens* Cultures

EPS	elemental composition (molar ratio with respect to total carbon)			chemical functions(molar ratio with respect to total carbon)							
	O/C	N/C	P/C	284.8 eV C–(C,H)	286.2 eV C–(O,N)	287.8 eV C=O– C–O	289.0 eV O=C– OHO=C–OR	531.3 eV O= CP=O	532.7 eV HO– CC–O–C	399.9 eV N _{nonpr}	401.3 eV N _{pr}
control (bound EPS)	0.607	0.285	0.004	0.417	0.367	0.176	0.040	0.206	0.401	0.261	0.024
BisBAL (bound EPS)	0.261	0.069	0.001	0.421	0.361	0.176	0.042	0.101	0.160	0.063	0.006
control (free EPS)	0.643	0.136	0.013	0.445	0.357	0.166	0.033	0.172	0.471	0.114	0.022
BisBAL (free EPS)	0.289	0.086	0.005	0.459	0.343	0.164	0.034	0.084	0.205	0.078	0.008

for these comparisons because it was most effective in suppressing EPS production.
The carbon peak was resolved into four component peaks (fwhm = 1.45 eV) and the peaks were assigned as follows: (1)

a peak at 284.8 eV attributed to C–(C, H) from lipids or amino acid side chains, (2) a peak at 286.2 eV is due to C–(O, N), associated with alcohol, ether, amine, or amide, (3) a peak at 287.8 eV is the result of C=O or O–C–O, like in carboxylate,

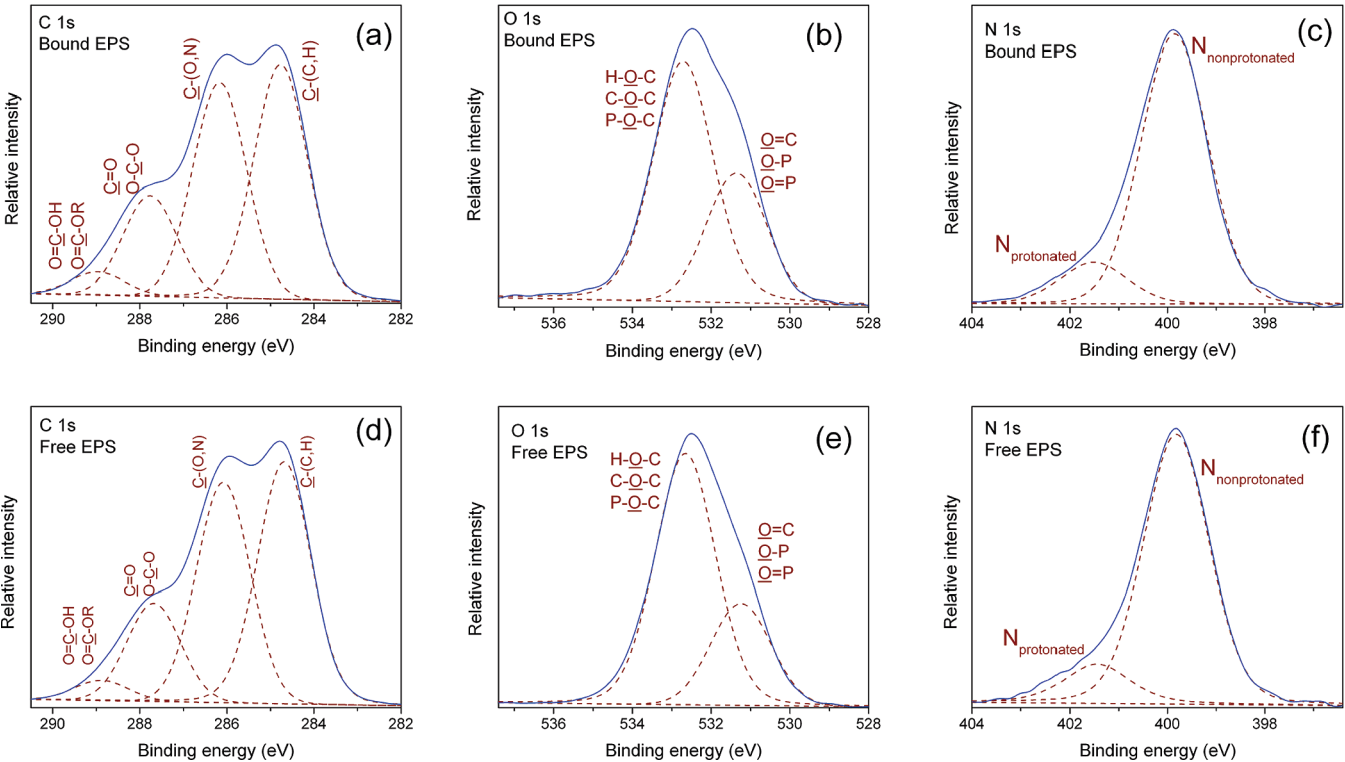


Figure 6. High resolution 1s XPS spectra of bound and free EPS from *S. marcescens* following 2 days of growth. Carbon, oxygen, and nitrogen from bound EPS are shown in (a), (b), and (c), respectively, whereas (d), (e), and (f) depict similar data for free EPS.

carbonyl, amide, acetal, or hemiacetal, and (4) a weak peak at 289.0 eV arises from $\text{O}=\text{C}-\text{OH}$ and $\text{O}=\text{C}-\text{OR}$, commonly found in carboxyl or ester groups. The infrared spectral band in the range $1741-1727\text{ cm}^{-1}$ (Figure 2a,b) confirm XPS peak assignment at 287.8 eV (Figure 6) suggesting that $\nu\text{C}=\text{O}$ of $\text{O}-\text{acetyl}$ ester bonds contribute significantly to both $\text{C}=\text{O}$ and $\text{O}-\text{C}-\text{O}$.

The O 1s peak was decomposed into two peaks (fwhm = 1.80 eV): (1) a peak at 531.3 eV is mainly due to $\text{Q}=\text{C}$, as in carboxylate, carbonyl, ester, or amide and (2) contribution from $\text{Q}-(\text{C}, \text{H})$, including hydroxide, acetal, and hemiacetal at 532.7 eV. Acetal, hemiacetal, and hydroxide indicate the presence of carbohydrates; carboxylate and carboxyl groups are likely due to proteins and acidic carbohydrates. The N 1s peak was also resolved into two component peaks (fwhm = 1.54 eV). The peak at 399.9 eV is solely due to nonprotonated nitrogen, N_{nonpr} , as in amines and amides, and the other peak at 401.3 eV is mainly from protonated amines, N_{pr} , which are likely from basic amino acids such as Lysine and Arginine.

The original peaks and the individually resolved ones from Figure 6 were numerically integrated to calculate concentration ratios, which are summarized in Table 5 for both free and bound EPS extracted from the control and BisBAL-treated samples. The calculated C, O, N, and P percentages for free and bound EPS were 56.0, 36.0, 7.6, and 0.7% and 52.7, 32.0, 15.0, and 0.2%, respectively, for the controls, which are in the range reported for sulfate-reducing bacteria⁵⁰ and *B. subtilis*.⁶ As expected, the elemental abundances in all EPS samples were $\text{C} > \text{O} > \text{N} > \text{P}$. Also, bound EPS in *S. marcescens* was richer in nitrogen-containing compounds compared with free EPS, which is consistent with the amide I band dominating the oxygen containing compounds in the $1200-900\text{ cm}^{-1}$ range in Figure 2a and in *B. subtilis*.⁶ After BisBAL treatment, the calculated C, O, N, and P percentages for free and bound EPS were 72.5, 20.9, 6.3, and 0.3% and 75.0, 19.6, 5.3, and 0.1%, respectively. Hence, consistent with the overall decrease in infrared absorbances with BisBAL treatment, XPS also demonstrates a reduction in the relative contributions of O and N to free and bound EPS.

Table 5 qualitatively verifies FTIR measurements in the sense that BisBAL treatment decreased EPS polysaccharides and proteins for free and bound EPS (as manifested by substantially lower O/C and N/C ratios), indicating that BisBAL may be effective for inhibiting bacterial aggregation as well as biofilm formation. Concentrations of phosphorus-containing compounds in both bound and free EPS were significantly lower than proteins and polysaccharides as shown by P/C ratios. Interestingly, even though BisBAL treatment decreased overall EPS production and simultaneously increased the percentage of total carbon, the ratios of component peaks to total carbon (at 284.8, 286.2, 287.8, and 289.0 eV) remained constant in all cases. Hence, the relative contributions of the individual carbon moieties constituting the deconvoluted peaks to the total amount of EPS expressed remained constant between free and bound EPS and were independent of BisBAL treatment.

$\text{C}_{286.2}$ molar ratios with respect to total carbon for bound and free EPS from *S. marcescens* are similar to *B. subtilis*⁶ and lie between the values reported for model proteins and polysaccharides.^{23,49} $\text{C}_{287.8}$ molar ratios obtained for every EPS sample (free and bound in the presence and absence of bismuth) were close to those reported for model polysaccharides (0.167) but lower than those for proteins (0.225–0.279).²³ Exposure of *S. marcescens* to BisBAL for 2 days decreased carboxylate, carbonyl, ester, or amide components ($\text{O}_{531.3}$ molar ratios) by

~50% in both bound and free EPS. Interestingly, acidic carbohydrates contributed more to free EPS in the absence of bismuth but to bound EPS in BisBAL treated cultures as evidenced by the higher $\text{O}_{531.3}$ molar ratios. $\text{O}_{532.7}$ ratios were always higher in free EPS than in bound EPS, indicating higher polysaccharide concentrations in free EPS. These XPS observations are supported by the dominant infrared spectral bands between 1200 and 900 cm^{-1} in Figure 2b compared with Figure 2a, confirming that free EPS is higher in concentrations of $\text{P}=\text{O}$ of phosphodiester (O 1s peak at 532 eV), $\text{C}=\text{O}$ groups, and polysaccharides. BisBAL treatment decreased carbohydrates attributed to $\text{O}_{532.7}$ by 60% in bound EPS and 56% in free EPS. In all cases, nonprotonated amines were approximately 1-order of magnitude higher in concentration compared with protonated amines. BisBAL was more effective in reducing amine production in bound EPS compared with free EPS.

Auger Electron Spectroscopy (AES). Secondary electron micrographs of EPS samples on the silicon substrate imaged during collection of Auger spectra revealed in all cases a uniform surface distribution of EPS that was essentially free of bacterial debris. Additionally, for each sample, the Auger spectrum, composed of the average of 10 separate collection cycles, were essentially indistinguishable from the initial collection cycle spectrum demonstrating that EPS was negligibly damaged by the electron beam during analysis.

Figure 7 shows the effects of bismuth thiols on Auger spectra of bound and free EPS of *S. marcescens* and *E. coli* cultures. Spectra were collected in the energy range 0–1100 eV, but only the range 0–600 eV is depicted because it encompassed the required elemental information. Spectra in the 600–1100 eV range were essentially devoid of features, except for Na, which was attributed to the media and buffers employed. The silicon peak was attributed to the silicon substrate employed and the chlorine peak was the result of NaCl employed for bound EPS extraction and in the *E. coli* growth media. As previously determined through XPS (Figure 5), C, N, O, and P were the major elemental components of EPS consistent with it being comprised mainly of carbohydrates, proteins, (phospho)lipids, and nucleic acids.^{1,2,16}

N, O, and P ratios with respect to C were obtained from Figure 7 and summarized in Table 6. As observed, all elemental ratios decreased in the presence of bismuth thiols demonstrating their ability to suppress EPS secretion as reported earlier in this manuscript from colorimetry, FTIR, and XPS. Comparing the O/C, N/C, and P/C ratios demonstrates that BisBAL was as good or better than the other two bismuth thiols at suppressing EPS secretion, which is also in agreement with colorimetry, FTIR, and XPS data. For both *S. marcescens* and *E. coli*, $(\text{N/C} + \text{O/C})$ ratios are greater in free EPS demonstrating that it is richer than bound EPS in nitrogen- and oxygen-containing compounds. Also, free EPS of *E. coli* is richer in phosphorus-containing compounds given the higher P/C ratios; with reference to Figure 3b,d, these compounds are probably proteins, phospholipids, phosphodiester, and nucleic acids. No phosphorus was detected in bound EPS of *S. marcescens*, indicating that it contains negligible amounts of phosphorylated compounds. Decreases in the elemental $(\text{N/C} + \text{O/C})$ ratios from AES (Table 6) and XPS (Table 5) also support decreases in secondary protein structures as observed in FTIR spectra (Table 4).

Even though Table 6 largely captures the trends obtained from FTIR spectra and XPS, decreases in elemental ratios with bismuth treatment did not quantitatively agree with trends obtained from FTIR band analysis and some O/C ratios did not match XPS results shown in Table 5. Because XPS and AES

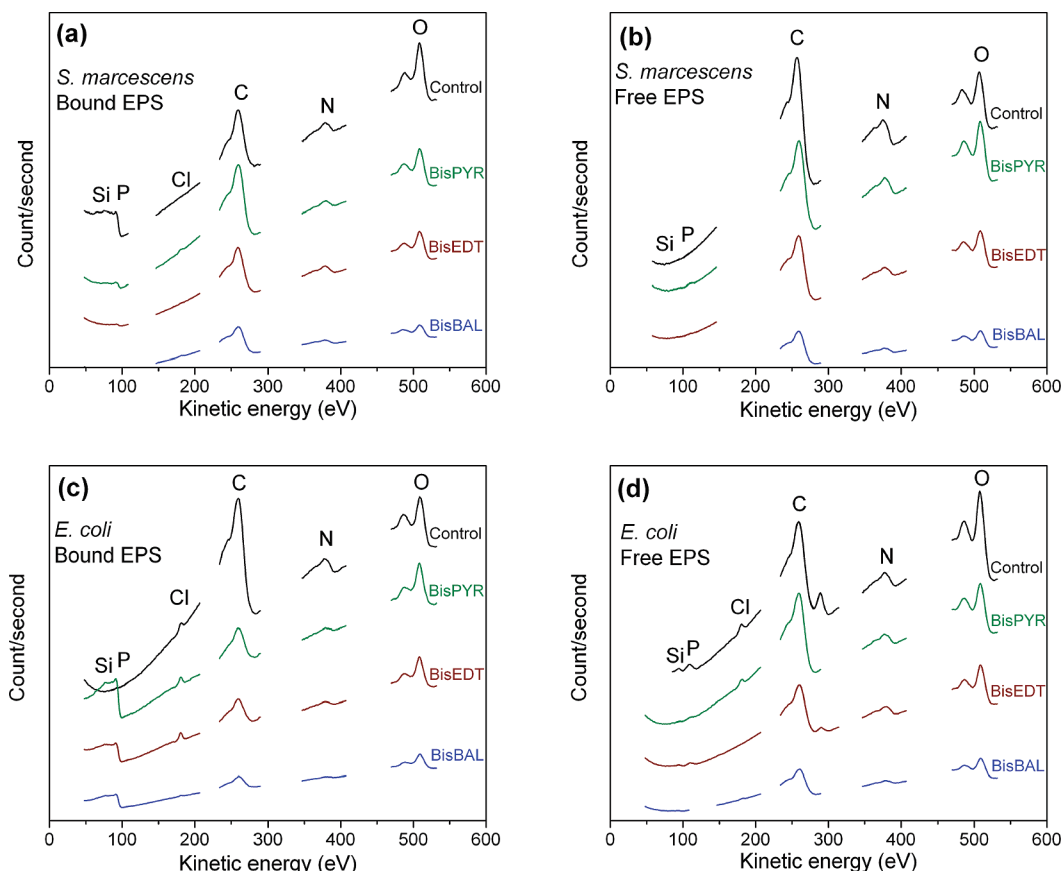


Figure 7. High resolution scanning Auger electron spectra of EPS extracted from stationary phase cultures of *S. marcescens* and *E. coli*. Spectra depict the effects of various bismuth thiols on the atomic composition of EPS. Bound and free EPS produced by *S. marcescens* after 2 days of incubation are shown in (a) and (b), respectively, and EPS produced by *E. coli* after 2 days of incubation are depicted in (c) and (d).

Table 6. Elemental Composition (Molar Ratios with Respect to Total Carbon) of Bound and Free EPS from *S. marcescens* and *E. coli* upon Exposure to Various Bismuth Thiols Following 2 Days of Incubation

	control (no bismuth)		BisBAL		BisEDT		BisPYR	
	<i>S. marcescens</i>	<i>E. coli</i>	<i>S. marcescens</i>	<i>E. coli</i>	<i>S. marcescens</i>	<i>E. coli</i>	<i>S. marcescens</i>	<i>E. coli</i>
Bound EPS from <i>S. marcescens</i> and <i>E. coli</i>								
N/C	0.109	0.079	0.058	0.081	0.097	0.098	0.085	0.077
O/C	0.472	0.223	0.253	0.620	0.317	0.646	0.249	0.649
P/C	not detected	0.001	not detected	0.003	not detected	0.004	not detected	0.006
Free EPS from <i>S. marcescens</i> and <i>E. coli</i>								
N/C	0.113	0.100	0.112	0.080	0.086	0.116	0.091	0.089
O/C	0.233	0.516	0.342	0.383	0.289	0.438	0.259	0.319
P/C	0.001	0.028	0.009	not detected	0.005	0.019	0.005	0.009

were performed using purified EPS from the same vial, discrepancies in elemental ratios indicates potential artifacts introduced during sample preparation. Limited operator control over spreading and drying of the liquid EPS drop on the silicon substrate could have contributed to analytical differences. It is also possible that oxygen signal from the substrate could have contributed to higher O/C ratios since the EPS films analyzed were fairly thin.

Conclusions

Differences were observed in the amounts and chemical compositions of free and bound EPS produced by suspended cultures of *S. marcescens* and *E. coli*: (1) higher amounts of total free EPS (polysaccharides + proteins) were secreted compared with total bound EPS, (2) free EPS was enriched in neutral carbohydrates, (3) amide II of proteins and nucleic acids

were present only in free EPS, (4) total nitrogen and oxygen containing compounds were richer in free EPS, and (5) acidic moieties with COO^- functionalities were present at higher levels in bound EPS.

EPS secretions were significantly decreased in the presence of minimum inhibitory concentrations of bismuth thiols (5 μM BisBAL, 2 μM BisEDT, and 7 μM BisPYR for *S. marcescens* and 11 μM BisBAL, 6 μM BisEDT, and 5 μM BisPYR for *E. coli*). Extensive characterization using FTIR, AES, and XPS suggests that antifouling properties of bismuth thiols arise from (1) inhibition of carbohydrate O-acetylation especially for *S. marcescens*, (2) specific losses of protein secondary structures including β -sheets and α -helices + unordered coils, and (3) an overall reduction in total (free + bound) EPS proteins and polysaccharides. Also, BisBAL appears to be more effective than other bismuth thiols for biofouling control since it achieved largest reductions in EPS production. Our observations should

be cautiously extrapolated to real-world systems for suppressing biofilm formation or bacterial aggregation because (1) antifouling capabilities of bismuth thiols toward mixed bacterial populations and their environmental toxicity and biodegradability have not yet been established and (2) different trends might be obtained for other concentrations and formulations of bismuth thiols.

Acknowledgment. This research has been funded by grants from the National Science Foundation CAREER program (CBET-0134301) and the Texas Hazardous Waste Research Center (066UHH2925). A portion of the research described in this manuscript was performed in the Environmental Molecular Sciences Laboratory, a national scientific user facility sponsored by the Department of Energy's Office of Biological and Environmental Research and located at Pacific Northwest National Laboratory. The contents do not necessarily reflect the views and policies of the sponsors nor does the mention of trade names or commercial products constitute endorsement or recommendation for use.

Supporting Information Available. Growth curves for *S. marcescens* and *E. coli* over a 6-day period (Figures S1a and S1b), epifluorescence photomicrographs of metabolically active and inactive cells (Figures S2 and S3), and measurements of live/dead cell counts (Tables S1 and S2) are provided. All data were obtained in the absence of bismuth thiols (control samples) and in the presence of sub MICs of bismuth thiols (5 μ M BisBAL, 2 μ M BisEDT, and 7 μ M BisPYR for *S. marcescens* and 11 μ M BisBAL, 6 μ M BisEDT, and 5 μ M BisPYR for *E. coli*). This material is available free of charge via the Internet at <http://pubs.acs.org>.

References and Notes

- Wingender, J.; Neu, T. R.; Flemming, H.-C. *Microbial Extracellular Polymeric Substances: Characterization, Structure and Function*; Springer: Berlin Heidelberg, 1999.
- Denkhaus, E.; Meisen, S.; Telgheder, U.; Wingender, J. *Microchim. Acta* **2007**, 158, 1–27.
- Eboigbodin, K. E.; Biggs, C. A. *Biomacromolecules* **2008**, 9 (2), 686–695.
- van der Aa, B. C.; Dufrêne, Y. F. *Colloids Surf. B* **2002**, 23, 173–182.
- Characklis, W. G.; Marshall, K. C. *biofilms*; John Wiley & Sons: New York, 1990.
- Omoike, A.; Chorover, J. *Biomacromolecules* **2004**, 5, 1219–1230.
- Tsuneda, S.; Aikawa, H.; Hayashi, H.; Yuasa, A.; Hirata, A. *FEMS Microbiol. Lett.* **2003**, 223, 287–292.
- Domenico, P.; Baldassarri, L.; Schoch, P. E.; Kaehler, K.; Sasatsu, M.; Cunha, B. A. *Antimicrob. Agents Chemother.* **2001**, 45 (5), 1417–1421.
- Domenico, P.; Salo, R. J.; Novick, S. G.; Schoch, P. E.; Van Horn, K.; Cunha, B. A. *Antimicrob. Agents Chemother.* **1997**, 41 (8), 1697–1703.
- Domenico, P.; Tomas, J. M.; Merino, S.; Rubires, X.; Cunha, B. A. *Infect. Immun.* **1999**, 67 (2), 664–669.
- Badireddy, A. R.; Chellam, S.; Yanina, S.; Gassman, P. L.; Rosso, K. M. *Biotechnol. Bioeng.* **2008**, 99 (3), 634–643.
- Zhang, H.; Tang, J.; Meng, X.; Tsang, J.; Tsang, T.-K. *Dig. Dis. Sci.* **2005**, 50 (6), 1046–1051.
- Wingender, J.; Neu, T. R.; Flemming, H.-C. In *Microbial Extracellular Polymeric Substances: Characterization, Structure and Function*; Springer: Berlin, Heidelberg, 1999; pp 1–19.
- Beech, I.; Hanjagssit, L.; Kalaji, M.; Neal, A. L.; Zinkevich, V. *Microbiology* **1999**, 145, 1491–1497.
- Omoike, A.; Chorover, J. *Geochim. Cosmochim. Acta* **2006**, 70, 827–838.
- Christensen, B. E.; Characklis, W. G. In *biofilms*; Characklis, W. G., Marshall, K. C. Eds.; John Wiley & Sons: New York, 1990; pp 93–130.
- Naumann, D.; Schultz, C. P.; Helm, D. In *Infrared Spectroscopy of Biomolecules*; Mantsch, H. H., Chapman, D. Eds. John Wiley & Sons: New York, 1996; pp 279–310.
- Naumann, D.; Helm, D.; Labischinski, H.; Giesbrecht, P. In *Modern Techniques for Rapid Microbiological Analysis*; Nelson, W. H. Ed.; VCH: New York, 1991; pp 43–96.
- Marley, L.; Signolle, J. P.; Amiel, C.; Travert, J. *Vib. Spectrosc.* **2001**, 26, 151–159.
- Verhoef, R.; Schols, H. A.; Blanco, A.; Siika-aho, M.; Rättö, M.; Buchert, J.; Lenon, G.; Voragen, A. G. J. *Biotechnol. Bioeng.* **2005**, 91 (1), 91–105.
- Beech, I. B. *Int. Biodeterior. Biodegrad.* **2004**, 53, 177–183.
- Tyler, B. J. *Ann. N. Y. Acad. Sci.* **1997**, 831 (1), 114–126.
- Rouxhet, P. G.; Mozes, N.; Dengis, P. B.; Dufrêne, Y. F.; Gerin, P. A.; Genet, M. J. *Colloids Surf. B* **1994**, 2 (1–3), 347–369.
- Ahimou, F.; Boonaert, C. J. P.; Adriaensen, Y.; Jacques, P.; Thonart, P.; Paquot, M.; Rouxhet, P. G. *J. Colloid Interface Sci.* **2007**, 309, 49–55.
- McArthur, S. L.; McLean, K. M.; St John, H. A. W.; Griesser, H. J. *Biomaterials* **2001**, 22 (24), 3295–3304.
- Jolley, J. G.; Geesey, G. G.; Hankins, M. R.; Wright, R. B.; Wichlacz, P. L. *Surf. Interface Anal.* **1988**, 11, 371–376.
- Huang, C.-T.; Stewart, P. S. J. *Antimicrob. Chemother.* **1999**, 44, 601–605.
- Kaper, J. B.; Nataro, J. P.; Mobley, H. L. T. *Nat. Rev. Microbiol.* **2004**, 2, 123–140.
- Hejazi, A.; Falkner, F. R. J. *Med. Microbiol.* **1997**, 46 (11), 903–912.
- Traub, W. H. *Chemotherapy* **2000**, 46, 315–321.
- Wu, C.-L.; Domenico, P.; Hassett, D. J.; Beveridge, T. J.; Hauser, A. R.; Kazzaz, J. A. *Am. J. Respir. Cell Mol. Biol.* **2002**, 26, 731–738.
- Kulkarni, P.; Chellam, S.; Mittlefehldt, D. W. *Anal. Chim. Acta* **2007**, 581 (2), 247–259.
- Sheng, G.-P.; Yu, H.-Q.; Yu, Z. *Appl. Microbiol. Biotechnol.* **2005**, 67, 125–130.
- Walker, S. L.; Hill, J. E.; Redman, J. A.; Elimelech, M. *Appl. Environ. Microbiol.* **2005**, 71 (6), 3093–3099.
- de Brouwer, J. F. C.; Wolfstein, K.; Stal, L. J. *Eur. J. Phycol.* **2002**, 37, 37–44.
- Schmitt, J.; Flemming, H.-C. *Int. Biodeterior. Biodegrad.* **1998**, 41, 1–11.
- Barth, A.; Zscherp, C. *Q. Rev. Biophys.* **2002**, 35 (4), 369–430.
- Maquelin, K.; Kirschner, C.; Choo-Smith, L.-P.; Ngo-Thi, N. A.; Naumann, D.; Puppels, G. J. *Vibrational Spectroscopic Studies of Microorganisms*, 1st ed.; John Wiley & Sons: Chichester, 2002; Vol. 5, pp 3308–3334.
- Buijs, J.; Norde, W.; Lichtenbelt, J. W. T. *Langmuir* **1996**, 12, 1605–1613.
- Stuart, B. H. *Infrared Spectroscopy: Fundamentals and Applications*; John Wiley & Sons Ltd: Chichester, West Sussex, 2004; p 224.
- Beamson, C.; Briggs, D. *High Resolution XPS of Organic Polymers: The Scienta ESCA300 Database*; John Wiley & Sons: Chichester, U.K., 1992; p 293.
- Hochella, J. M. F.; Harris, D. W.; Turner, A. M. *Am. Mineral.* **1986**, 71, 1247–1257.
- Baer, D. R.; Engelhard, M. H.; Lea, A. S. *Surf. Sci. Spectra* **2003**, 10, 1–10.
- Childs, K. D.; Carlson, B. A.; LaVanier, L. A.; Moulder, J. F.; Paul, D. F.; Stickle, W. F.; Watson, D. G. *Handbook of Auger Electron Spectroscopy: A Book of Reference Data for Identification and Interpretation in Auger Electron Spectroscopy*, 3rd ed.; Physical Electronics: Eden Prairie, 1995.
- Han, L.; Enfors, S.-O.; Häggström, L. *Bioprocess Biosyst. Eng.* **2003**, 25, 205–212.
- Lin-Vien, D.; Colthup, N. B.; Fateley, W. G.; Grasselli, J. G. *The Handbook of Infrared and Raman Characteristic Frequencies of Organic Molecules*; Academic Press, Inc.: San Diego, 1991.
- Nivens, D. E.; Ohman, D. E.; Williams, J.; Franklin, M. J. *J. Bacteriol.* **2001**, 183 (3), 1047–1057.
- Neu, T. R.; Marshall, K. C. *Biofouling* **1991**, 3, 101–112.
- Dufrêne, Y. F.; Boonaert, C. J. P.; Rouxhet, P. G. In *Methods in Enzymology: biofilms*; Doyle, R. J. Ed.; Academic Press: London, U.K., 1999; Vol. 310, pp 375–389.
- Chan, K.-Y.; Xu, L.-C.; Fang, H. H. P. *Environ. Sci. Technol.* **2002**, 36, 1720–1727.